Vision Res. Vol. 14, pp. 1475–1482. Pergamon Press 1974. Printed in Great Britain.

TECHNICAL NOTE

ALOPEX: A STOCHASTIC METHOD FOR DETERMINING VISUAL RECEPTIVE FIELDS

E. HARTH[1] and E. TZANAKOU
Physics Department, Syracuse University, Syracuse, New York 13210, U.S.A.

(*Received* 17 *January* 1974)

1. SINGLE NEURON RECEPTIVE FIELDS

Although information, processed in the central nervous system, is likely to be reflected in the global behavior of large numbers of neurons, practical experimental limitations force the physiologist to seek meaning and function in the firing records of single neurons. In particular, the concept of a *receptive field* has become a key in our understanding of sensory information processing. Originally denoting merely that region of sensory space which affects a particular neuron (Hartline, 1940), the discovery of complex and hypercomplex cells necessitated a redefinition. For the case of the visual pathway, with which we will be exclusively concerned, we may define receptive field as that spatio-temporal stimulus pattern, or class of patterns, which maximally affects the firing rate of a given neuron. Such a pattern may, in the case of neurons in the mammalian retina, consist simply of a small disc of light in a specific location, against a darker background (Kuffler, 1953). In other animals, instead of merely transmitting a "mosaic of impulses", the retinal network performs more elaborate transformations on the projected image. This appears to be the case in the frog retina (Lettvin *et al.*, 1959). In the mammalian visual cortex Hubel and Wiesel have found a variety of linear field structures, which they divided into *simple*, *complex* and *hypercomplex* fields (Hubel and Wiesel, 1959, 1962, 1968). The latter include not only the spatial, but also the temporal dependence of light distribution, e.g. motion in a particular direction. In principle, any visual event or sequence of events displayed on the retina may be the receptive field of a particular neuron. It is a frequently made hypothesis, though by no means self-evident, that such neurons function as *detectors* of the specific sensory *trigger features* defined by their receptive fields (Barlow, Narasimhan and Rosenfeld, 1972).

Under this hypothesis the perception of a sensory event, such as a horizontal bar of light, is equivalent to stimulating to a high firing rate those neurons for which that sensory event is the receptive field.

2. CURRENT EXPERIMENTAL METHODS

Procedures in use for determining visual receptive fields fall into two general categories: (a) a small test spot of light is used to explore and map the excitatory and inhibitory portions of the field; and (b) the response of a neuron is recorded for different trial patterns presented to the organism.

Recording of the cell's response (to each position of the test spot, or trial pattern) is accomplished by means of intracellular or extracellular microelectrodes. The *response* comprises in principle the detailed firing record of the cell. In practice, the physiologist will fix his attention on statistical parameters such as latency and average firing frequency at different time intervals following the stimulus.

Both methods have produced a wealth of scientific information. They are, however, quite limited in their applicability, each for different reasons. Procedure (a) can be used to obtain detailed field patterns. It has the advantage of being independent of preconceived notions concerning the optimal stimuli. On the other hand, the procedure is laborious, requiring many data points to form the required composite map. This limitation has been overcome, in part, by the application of computer technology to receptive field plotting (Spinelli, 1966, 1967). In this method a small disk of light is driven repeatedly across a matrix of sampling points, while an on-line computer records and accumulates the counts received for each sampling point.

Unfortunately, the method of exploring the field by a small illuminated spot cannot always be used. It is particularly inapplicable to the so called complex and hypercomplex fields, which are no longer stationary maps consisting of well defined excitatory and inhibitory regions. Such cells generally exhibit little or no response to stimulation by a single small spot. Through very painstaking work in the cat and monkey visual cortex, Hubel and Wiesel have, by using procedure (b), succeeded in cataloguing a great variety of receptive fields. These consist of simple geometrical patterns such as bars and edges of light, with or without motion. Indications are that these field patterns become more complicated as one proceeds toward higher brain centers, and soon reach a degree of complexity that makes detection of a receptive field a rare experimental accident. The report of Gross, Bender and Rocha-Miranda (1969) who—upon exploring the inferotemporal cortex of a monkey—found a neuron that responded preferentially to the pattern of a monkey's hand, must be viewed as such a chance event. It is significant in providing evidence that such complicated and highly specialized field patterns exist, but no one has suggested to make a systematic study of such fields with present experimental techniques.

[1] This author wishes to acknowledge the hospitality of the Aspen Center for Physics during the summer of 1973.

In summary, the limitations of current techniques are set, on the one hand, by the limits of applicability of method (a), and, on the other, by the nature of method (b), which requires a guessing of the approximate parameters defining a receptive field, and thus becomes inapplicable for all but the simplest field contours.

3. ALOPEX[2]

A method has been developed in this laboratory (Harth and Tzanakou, 1972; Tzanakou and Harth, 1973) which should avoid the difficulties of both classical methods. As presently conceived, it should be applicable to simple, as well as to some complex and hypercomplex cells. The fundamental idea rests on the assumption that a stimulus pattern resembling the receptive field of a cell, will produce responses which approach the optimal response, as this resemblance increases.

This allows one to devise an algorithm which compares responses to different trial patterns, and generates a new trial pattern. The algorithm is carried out by a computer, which receives information concerning the cell's response and, in turn, controls the pattern of light presented to the animal. This iterative procedure starts with a completely random pattern.

In this paper we present a brief description of the new principles involved, the results of some computer simulations, designed to test the feasibility of the method, and an outline of the instrumentation with which we are now implementing the method.

Presentation of these preliminary data is in response to a number of requests to make the method available to other investigators, who may have better research facilities in the field of sensory physiology.

Algorithm. We consider a screen divided into N^2 elements, making N rows and N columns, and numbered consecutively from 1 to N^2. Let the light be uniform over each square element, and denote the intensity of light at the jth element by i_j. Time is divided into successive intervals τ. A stationary pattern of light $\mathbf{I}(n)$ is presented during the nth time interval, where

$$\mathbf{I}(n) = \begin{pmatrix} i_1(n) \\ \cdot \\ \cdot \\ \cdot \\ i_{N^2}(n) \end{pmatrix}. \tag{1}$$

With each presentation of the light pattern $\mathbf{I}(n)$, the response $R(n)$ of a neuron in the visual pathway is recorded. This *response* will in general be the number of action potentials accumulated in an appropriately chosen time interval. Each pair of light pattern and response, $\mathbf{I}(n)$ and $R(n)$, represents one *iteration* in the procedure.

[2] Acronym for: Algorithmic Logic of Pattern Extracting Crosscorrelations.

A quantity $P_j(n)$ is determined at each iteration n and for each element of space j according to:

$$\begin{aligned}
P_j(n) \quad &= 1 \quad \text{if} \quad R(n-1) > R(n-2) \text{ and } i_j(n-1) > i_j(n-2) \\
&\quad \text{or if} \quad R(n-1) < R(n-2) \text{ and } i_j(n-1) < i_j(n-2) \\
&= 0 \quad \text{if} \quad R(n-1) = R(n-2) \text{ or } i_j(n-1) = i_j(n-2) \\
&= -1 \quad \text{if} \quad R(n-1) < R(n-2) \text{ and } i_j(n-1) > i_j(n-2) \\
&\quad \text{or if} \quad R(n-1) > R(n-2) \text{ and } i_j(n-1) < i_j(n-2)
\end{aligned} \tag{2}$$

In words, the *parity* $P_j(n)$ is taken as $+1$, whenever response and light intensity have changed in the same direction; $P_j(n) = -1$ if R and i_j have changed in opposite directions, and $P_j(n) = 0$ if either or both have remained unchanged.

These parities are now used to determine the new intensities $i_j(n)$ in the following manner: The intensities $i_j(n)$ shall be proportional to the sum of a *bias* $b_j(n)$ and a random variable $r_j(n)$

$$i_j(n) = \nu(n)\,[b_j(n) + r_j(n)] \tag{3}$$

where $\nu(n)$ is a normalization constant, satisfying the condition that the light intensity, integrated over the entire visual space, be constant:

$$I = \sum_i i_i(n). \tag{4}$$

The biases $b_j(n)$ are given by

$$\left.\begin{aligned} b_j(n) &= b_j(n-1) + \beta P_j(n) \\ b_j(0) &= b_j(1) = 0 \text{ for all } j \end{aligned}\right\} \tag{5}$$

Here β is a positive constant. Equations (5) specify that the bias changes from one iteration to another by an amount $\pm\beta$ or 0, depending on which one of the conditions (2) is satisfied, and that the bias at any time $t = n\tau$ is the sum of the increments

$$b_j(n) = \beta \sum_{l=2}^{n} P_j(l). \tag{6}$$

Further, equations (3) and (5) indicate that the first two trial patterns $\mathbf{I}(0)$ and $\mathbf{I}(1)$ are completely random. From the intensities $i_j(0)$ and $i_j(1)$ and the responses $R(0)$ and $R(1)$ the first set of parities $P_j(2)$ is obtained, hence the summation in equation (6) starts with $l = 2$.

Dynamics of ALOPEX

The time course of events can be predicted for simple receptive fields, and under the assumption of a linear superposition of the contributions from different parts of the field. Such superposition has been assumed in several theoretical models (Ratliff, 1965; Harth and Pertile, 1972) and received some empirical justification (Kuffler, 1953; Rodieck and Stone, 1965).

Thus, assume that the illumination $i_j(n)$ contributes an amount

$$R_j(n) = [i_j(n)]^a \cdot \phi_j \tag{7}$$

to the response of the cell. ϕ_j will be called the *field strength* of the jth element; it is positive for excitatory, negative for inhibitory portions of the field, and zero for elements lying outside the receptive field.

We believe that the question, whether or not the response to light intensity follows a power law, as Stevens suggested (1970) or the classical Weber–Fechner relation, or some other function is not crucial to our argument. We have assumed the power law in equation (7) for the purpose of our computer simulations.

The response $R(n)$ of the neuron to the nth stimulus pattern will then be

$$R(n) = \sum_j R_j(n) = \sum_j [i_j(n)]^a \cdot \phi_j. \tag{8}$$

The series $\{i_j(n)\}$, $\{b_j(n)\}$, and $\{R(n)\}$ are interrelated, *non-stationary*, or *evolutionary stochastic processes*. They are also non-Markovian. In the computer simulations we have attempted to predict the evolution of these quantities, as they would occur in an actual experiment.

The algorithm described is designed to take advantage of the cross correlations that must exist between the changes of illumination, $i_j(n-1) - i_j(n-2)$, the jth element in space, and the change in neural response, $R(n-1) - R(n-2)$. The covariances (see for example Bartlett, 1962) i.e. the expectation values of these correlations, should be positive for excitatory, and negative for inhibitory portions of the field, as well as for regions lying outside the receptive field. In the last case the covariances would be zero, if it weren't for the normalization condition (4).

The effect of the algorithm expressed by equations (1–6) is thus to increase the light intensity in the excitatory regions, and decrease it everywhere else.

The normalization condition (equation 4) also allows one to define a set of optimal solutions for $\mathbf{I}$, call them $\{\mathbf{I}_{max}\}$, such that the corresponding responses are largest. Since $\mathbf{I}$ is a vector in N^2-space, and is constrained by equation (4) to lie in a hyperplane of $(N^2 - 1)$ dimensions, we can think of the response R to be a function of position within this hyperplane. Our algorithm thus constitutes a search for peaks in the hypersurface $R(\mathbf{I})$.

The effect of *compression* or *expansion* of the response, as function of light intensity, can be seen by assuming different values for the exponent a in equation (7). We give, for the sake of illustration, the following simple example. Let the excitatory portion of the receptive field consist of just three elements, having identical field strengths $\phi_1 = \phi_2 = \phi_3 = 1$. In Fig. 1(a) the triangle represents the plane $I = i_1 + i_2 + i_3 = 1$, and the schematic diagrams 1(b), 1(c) and 1(d) show the surfaces $R(\mathbf{I})$ for $a = 1$, $a < 1$, and $a > 1$ respectively. It is seen that in the first case *any* pattern, which distributes the amount of light I among the three excitatory elements of the field, yields the same response. For $a < 1$ equation (7) causes a *compression*, and equation (8) shows that the response will be greatest if the illumination is evenly distributed over the three

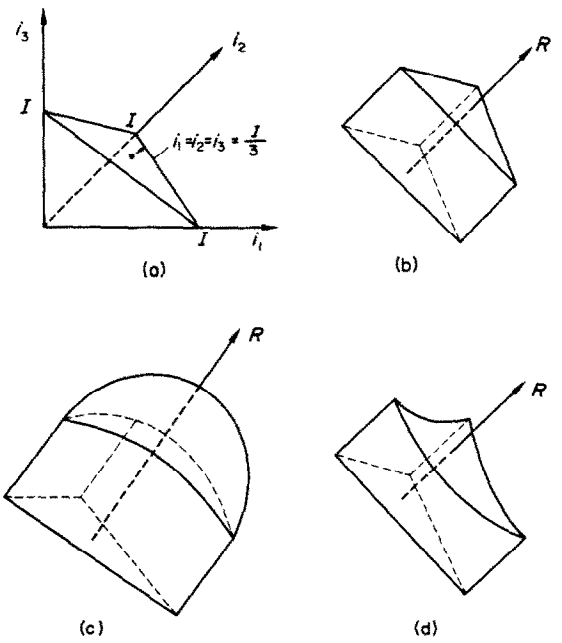

Fig. 1. Schematic diagram showing the linear superposition of responses for three field elements: (a) distribution of available light intensity I among the three field elements shows the *surface* of possible light distributions, here a plane equilateral triangle, whose center denotes a flat distribution across the field; (b) response R as function of light distribution, assuming the three field elements to have the same positive *field strength* ϕ, and assuming $a = 1$ in equations (7) and (8); (c) the effect of compression of the response ($a < 1$); maximal response for flat light distribution over the excitatory field; (d) the effect of $a > 1$ is that the flat distribution gives a minimum; peak responses occur for the cases of all light concentrated on any *one* of the three field elements.

field elements. On the other hand, if the response is *expanded* ($a > 1$), the surface for $R(\mathbf{I})$ will have three peaks, corresponding to all of the available light being concentrated on *one* of the three field elements [Fig. 1(d)].

A simple linear receptive field, of the type Hubel and Wiesel have reported for the mammalian visual cortex (Hubel and Wiesel, 1959, 1962, 1968) is probably due to the superposition of circular, on-center fields found at lower centers of the visual pathway. Compression of the response ($a < 1$ in the case of a power law), would then produce maximal response, if a given amount of light is distributed evenly along the linear field, rather than being concentrated in any one portion. Such a cell will act as a detector of a bar of light of specific location and orientation. A complex field, in which maximal response is elicited by a single bar of light of specific orientation but unspecified position in the field, may be due to superposition of similarly oriented line detectors. This is shown schematically in Fig. 2. Here the series of adjoining narrow rectangles represents the simple fields

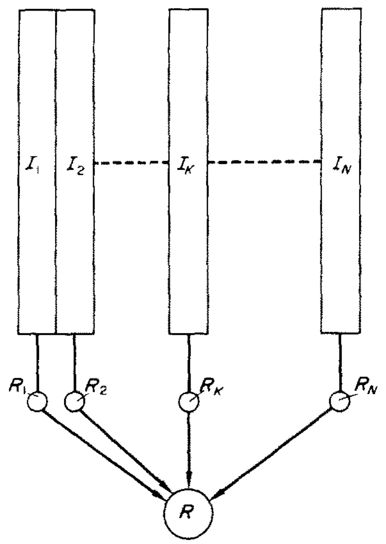

Fig. 2. Schematic diagram of the superposition of N responses R_k to form a *complex* response R. Here R_k is the response to an oriented bar of light I_k. It is assumed that the N simple fields are parallel, adjoining bars of light.

of cells, whose responses to illuminations $I_1 \ldots I_n$ are $R_1 \ldots R_n$ respectively. These, in turn, constitute the inputs to a complex cell. If the response R of that cell again follows a power law

$$R = C \sum_{k=1}^{N} R_k^b, \tag{9}$$

then, for b sufficiently large, maximal response is achieved by having all available light concentrated on *any one* of the narrow rectangular fields.

Column No.	1	2	3	4	5	6	7	8	9	10
	0	0	0	0	0	−20	40	−20	0	0
	0	0	0	0	0	−20	40	−20	0	0
	0	0	0	0	0	−20	40	−20	0	0
	0	0	0	0	0	−20	40	−20	0	0
	0	0	0	0	0	−20	40	−20	0	0
	0	0	0	0	0	−20	40	−20	0	0
	0	0	0	0	0	−20	40	−20	0	0
	0	0	0	0	0	−20	40	−20	0	0
	0	0	0	0	0	−20	40	−20	0	0
	0	0	0	0	0	−20	40	−20	0	0

Fig. 3. Assumed matrix of field strengths in computer simulation of a simple, excitatory, linear field with inhibitory surround.

4. COMPUTER SIMULATIONS

In order to check the feasibility of the proposed system, we have undertaken a series of computer simulation studies. In these the computer not only carries out the algorithms described above, but also computes the response of a model neuron having an assumed receptive field.

The functioning is seen from a simple example, in which we have assumed a visual space composed of a matrix of 10 × 10 elements. Ten of these are excitatory, forming a linear array, with an *inhibitory surround* of twenty elements (Fig. 3), thus simulating a simple cortical field. The field values ϕ_i are chosen in such a way that diffuse illumination over the entire receptive field would produce no change in the response of the neuron. The values for the illumination of the jth space element i_j are obtained at every iteration from equation 3. For $r_j(n)$ we used randomly chosen integers between 0 and 9; $b_j(n)$ was obtained from equation 6. Different values of β were tried. In the example shown here β was equal to 5, i.e. the bias increment was taken to be equal to the average random number in equation 3.

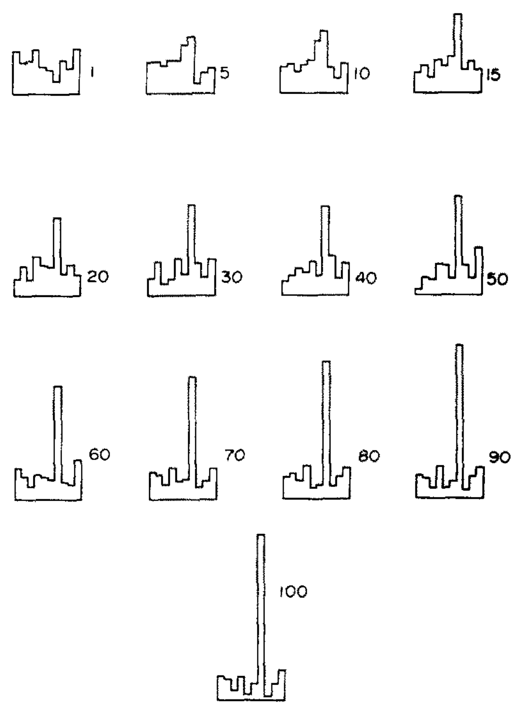

Fig. 4. Results of computer simulation of field shown in Fig. 3. The histograms show the distribution of illuminations, summed over the columns, and plotted as function of the column indices 1–10. Numbers above histograms refer to number of iteration. The first histogram is the result of the random pattern resulting from equation (3) when all biases are zero. Emergence of the 7th column begins around the 5th iteration and becomes more and more pronounced, as the process is continued.

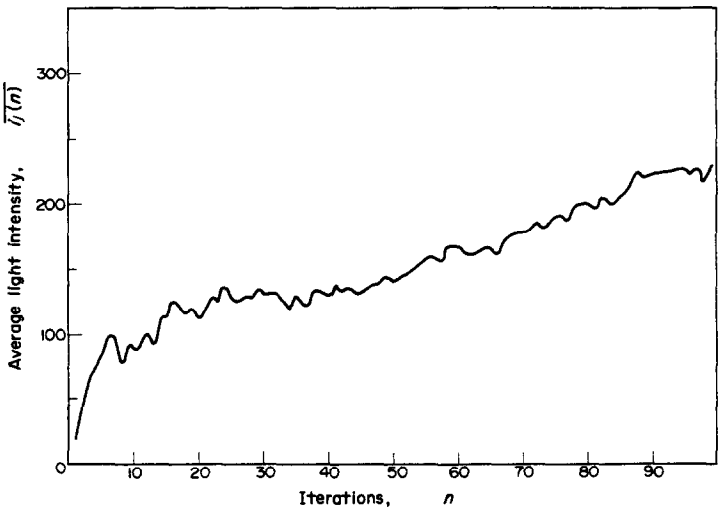

Fig. 5. Average values $\overline{i_j(n)}$ of illumination vs iteration n, taken over the ten excitatory elements (column 7). Illumination in this area is seen to increase progressively.

The responses were computed from equation (8). A value of 1 was chosen for a; the values of ϕ_j are those tabulated in Fig. 3.

Results of the computer simulation are shown in Fig. 4. The histograms give the values of the illuminations, summed over the ten elements in each column in the 10 × 10 array. Here the 7th column corresponds to the excitatory portion, columns 6 and 8 to the inhibitory portion of the field. All other columns lie outside the receptive field.

The first trial stimulus shows the random distribution resulting from equation (3) when all biases are zero. As early as the 5th iteration, the 7th column begins to emerge from the general background, and stands out clearly from the 15th iteration on. The rise of illumination in the excitatory region occurs at the expense of the background light, as required by the normalization condition. This is also illustrated in Fig. 5, where we have plotted the time course of the average illuminations $\overline{i_j(n)}$ for elements in the excitatory portions of the field, and in Fig. 6 in which the time course for all other elements is shown (solid line). In this graph we show also the illumination averages for inhibitory elements (dotted line). These are seen to drop significantly faster than the general background.

The gradual differentiation of the initially random

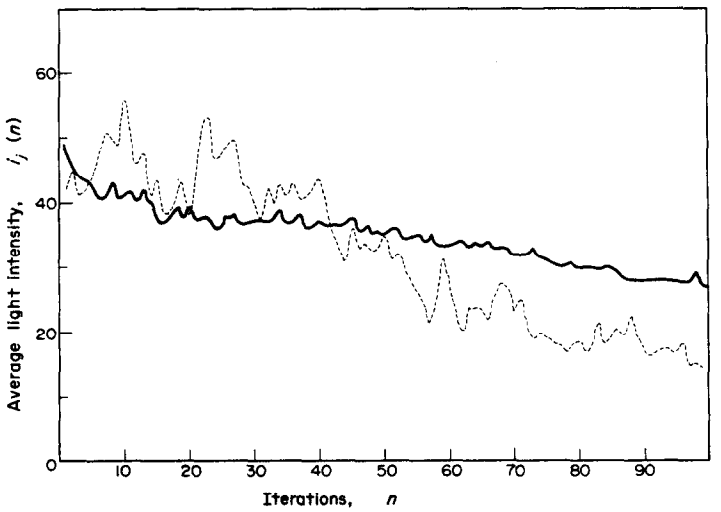

Fig. 6. Average values $\overline{i_j(n)}$ of illumination vs iteration n, taken over all non-excitatory elements (solid line), and over all inhibitory elements (dotted line). The progressive decline in illumination is slightly more pronounced for the inhibitories.

	Columns									
	1	2	3	4	5	6	7	8	9	10
Simple fields	−20	40	−20	0	0	0	0	0	0	0
	−20	40	−20	0	0	0	0	0	0	0
F_1	.	.	.							.
	.	.	.							.
	.	.	.							.
	−20	40	−20	0	0	0	0	0	0	0
	0	−20	40	−20	0	0	0	0	0	0
	0	−20	40	−20	0	0	0	0	0	0
	.	.	.							.
F_2	.	.	.							.
	.	.	.							.
	0	−20	40	−20	0	0	0	0	0	0
	.									
	.									
	.									
	.									
	.									
	0	0	0	0	0	0	0	−20	40	−20
	0	0	0	0	0	0	0	−20	40	−20
F_8	.	.	.							.
	.	.	.							.
	.	.	.							.
	0	0	0	0	0	0	0	−20	40	−20

Fig. 7. Assumed matrices of field strengths of eight simple, excitatory, linear fields. The fields are parallel and adjoining, their superposition producing a complex field as diagrammed in Fig. 2.

light pattern is accompanied by a continuous rise in the response function $R(n)$. Since no power law *compression* was used in the relationship between response and illumination, the asymptotic stimulus pattern tends to be uneven. The values for i_j (100) for elements in the 7th column and at the 100th iteration were 33, 8, 18, 26, 28, 24, 39, 18, 21 and 30.

We have attempted also to simulate complex receptive fields. In one such trial we used a superposition of eight simple linear fields, such as the one shown in Fig. 3. They differed in that each had the excitatory column in different adjacent locations from columns 2 through 9. This is sketched in Fig. 7. The outputs of these simple fields are superposed, as indicated in Fig. 2, and in accordance with equation (9). For the component simple fields we have again omitted the Stevens compression ($a = 1$). A superposition of the eight fields with the exponent $b = 1$ in equation (9), would then mean that, with the exception of the left and right borders of the 10×10 array, every element would have an effective field strength $\phi = 0$. Elements in columns 1 and 10 would be inhibitory with $\phi_j = -20$, those in columns 2 and 9 excitatory with $\phi_j = 20$. Apart from these *edge effects* the field would be *empty* and *simple*. For $b > 1$, however, no such elemental field strengths can be defined. The optimal light distribution is a vertical bar covering a *single* column, which may be any column from 2 to 9. The field is evidently complex.

In the present computer simulation we have chosen $b = 2$. The algorithm defined previously is now applied to the response of the complex cell. We show again the column sums of the illuminations for different iterations between 1 and 100 (Fig. 8). Note that the initial random pattern, labeled 1, has the same distribution as the one in Fig. 4, since the same random generator and starting values were used. Unlike in the previous run, however, the development is now strongly governed by statistical fluctuations. The system picks out of the noise what comes closest to looking like a line, and makes it into a line. Figure 8 shows that by the 10th iteration the 2nd column has emerged, with column 8 the closest competitor. By the 20th iteration the 8th column has gained the upper hand. This dominance is maintained and further reinforced over the next 80 iterations. The strong emergence of column 8 is, of course, fortuitous. Small variations in parameters, or a change in the starting value of the random generator will bring out different single columns. Also, if the exponent b in equation (9) is reduced to unity, a flat pattern is obtained.

Convergence characteristics of the procedure depend on many factors. The balance between the random and the feedback contributions to the illuminations [equation (3)] is critical. Preliminary results indicate an optimal value for β in equation (5) in the neighborhood of the average of the random variable $r_j(n)$. Another variable is the type of distribution chosen for $r_j(n)$. We have tried both flat and normal distributions of integers in the interval 0–9.

The covariances between $i_j(n)$ and the responses $R(n)$ depend strongly on the number of nonvanishing field values ϕ_j, but *not* on the number of elements outside the receptive field. This means that, for receptive fields subtending small solid angles, large areas can be

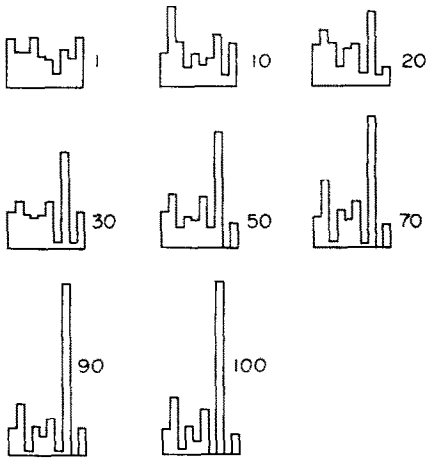

Fig. 8. Results of computer simulation of complex field shown in Fig. 7. Meaning and labeling of the histograms is the same as in Fig. 4. Starting with the same random pattern of illumination (iteration 1), *one* of the linear fields is seen to emerge in the final pattern.

explored with good convergence. On the other hand, large receptive fields may require many iterations, if good resolution is desired.

Although it is very likely that the type of complex field we have attempted to simulate, comes about through a superposition of fields as sketched in Fig. 2, it is not at all clear that the power law coupling described by equation (9) applies. If it does, the value of the exponent b is even less certain, except that it must be greater than 1. It is thus impossible to say, how closely these simulations resemble their counterparts in living systems. We believe to have shown, however, that our method has an excellent chance of being able to determine simple, and at least some of the complex visual receptive fields. The true potentialities and limitations of the method can only be determined in animal experimentations, some of which are now being carried out at this laboratory.

5. INSTRUMENTATION

The schematic diagram in Fig. 9 shows a simple system incorporating the new principles. It is now being tested in this laboratory by applying it to a receptive field study in the frog retina.

The system consists of a television screen (1), on which a matrix of 32 × 32 squares can be displayed. Light intensity in each square is set by a memory storage in the electronic device (2), which also controls the timing of the display. Each storage location in the memory holds four bits, thus providing 16 different levels of brightness for each element on the TV screen.

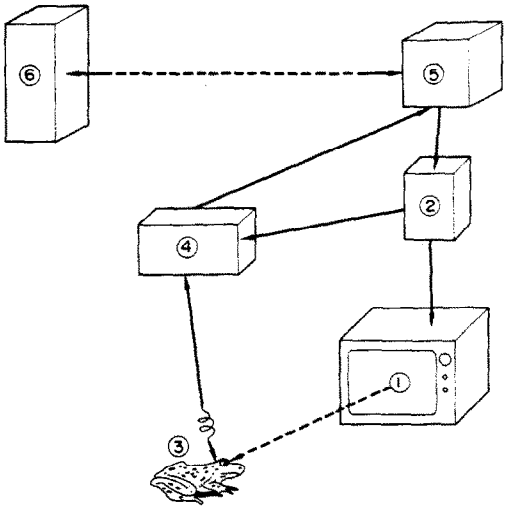

Fig. 9. Diagram of apparatus used in first application of ALOPEX process in receptive field studies of frog optic tectum: (1) television screen viewed by frog; (2) pattern memory and time sequencer; (3) microelectrode; (4) response integrator; (5) teletype and telephone coupler; (6) PDP-10 computer.

A single fiber is monitored in the optic tectum of a frog by a tungsten microelectrode (3). The amplified output is fed into the response integrator (4), which counts pulses within time intervals selected by the memory and time sequencer (2). This integrated output is transmitted via a teletype unit and telephone coupler (5) to a PDP-10 digital computer (6). The computer is

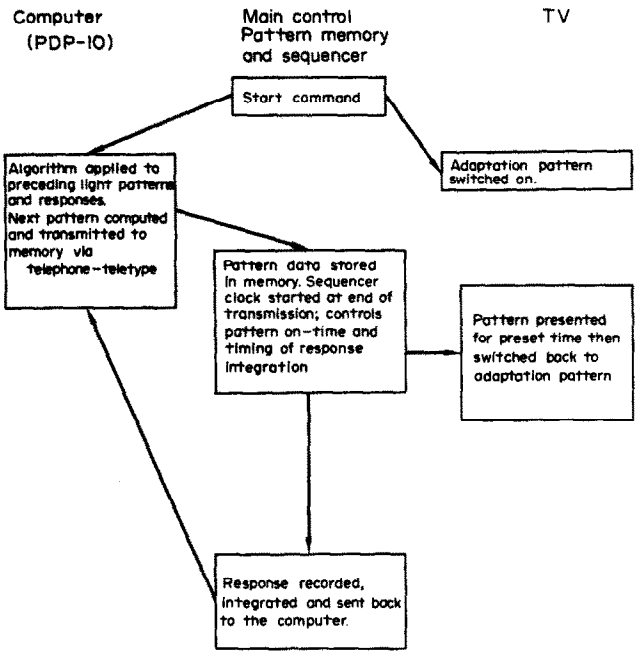

Fig. 10. Schematic of flow of information in ALOPEX system.

programmed to carry out all of the algorithms previously described, and transmits a new pattern of light intensities to the TV screen by way of the same telephone–teletype unit (5) and local memory storage (2).

With the present system the cycling rate is limited by the capacity of the 110 baud communication link with the computer, over which the 4096 bits of information that specify each pattern must be transmitted.

Timing of the test pattern and the period of response integration can be set to optimize counting statistics. This is achieved by proper allowance for latencies and adaptation, and by repeated presentation of the same pattern when necessary. Between presentations of the light patterns the TV screen is programmed to show even illumination across the entire face. The brightness of this *adaptation pattern* is preset by four binary switches, providing a choice of 16 intensity levels. A diagram of the flow of information in the system is shown in Fig. 10.

6. SUMMARY AND CONCLUSIONS

A method has been described for the determination of visual receptive fields by the use of an evolutionary stochastic process. Computer-generated light patterns evoke responses from single neurons in the visual pathway, which, in turn, modify the next light pattern by an algorithm, designed to cause convergence upon an optimal pattern of illumination. Feasibility was demonstrated in a series of computer simulation experiments, and a small system for animal experimentation has been constructed. The potentialities and limitations of the method can only be determined by applying the method to a variety of living systems. The authors hope that this paper will encourage such experiments.

ALOPEX has some interesting properties that may be explored in fields other than visual receptive field studies. It is a method of testing the performance of any pattern recognition device, and, in its most general aspect, a random search procedure for locating extrema in multidimensional surfaces. It is required, of course, that the extremum have a *ramp*, producing detectable changes in response, as the extremum is approached. This may be contrasted with the response of an ideal combination lock, which would be ALOPEX-resistant.

It should be clear also, that the ALOPEX process lends itself to many variations, beyond the relatively crude algorithm described in this paper. As an example, motion can be introduced in the search for visual receptive fields, by interposing movable prisms between the TV screen and the experimental animal. For pure translation, this would introduce two more variables, the velocities v_x and v_y, each determined by a random variable and a cumulative bias that, in turn, is controlled by feedback of the animal's response, in the manner indicated in equation (3).

Acknowledgements—The authors wish to thank Drs. Robert B. Barlow and Joseph F. Sturr for many helpful discussions, and for their expert advice in the field of sensory physiology.

REFERENCES

Barlow H. B., Narasimhan R. and Rosenfeld A. (1972) Visual pattern analysis in machines and animals. *Science, N.Y.* **177**, 567–575.

Bartlett M. S. (1962) *Stochastic Processes*. Cambridge University Press, Cambridge.

Gross C. G., Bender D. B. and Rocha-Miranda E. C. (1969) Visual receptive fields in inferotemporal cortex of the monkey. *Science, N.Y.* **166**, 1303–1305.

Harth E. and Tzanakou E. (1972) Stochastic method for computer-aided determination of visual receptive fields. Europ. Meeting of Cybernetics and Systems Res. Abstract 45. Vienna.

Harth E. and Pertile G. (1972) The role of inhibition and adaptation in sensory information processing. *Kybernetik* **10**, 32–37.

Hartline H. K. (1940) The receptive fields of optic nerve fibers. *Am. J. Physiol.* **130**, 690–699.

Hubel D. H. and Wiesel T. N. (1959) Receptive fields of single neurones in the cat's striate cortex. *J. Physiol.* **148**, 574–591.

Hubel D. H. and Wiesel T. N. (1962) Receptive fields, binocular interaction and functional architecture in the cat's visual cortex. *J. Physiol.* **160**, 106–154.

Hubel D. H. and Wiesel T. N. (1968) Receptive fields and functional architecture of monkey striate cortex. *J. Physiol.* **195**, 215–243.

Kuffler S. W. (1953) Discharge patterns and functional organization of mammalian retina. *J. Neurophysiol.* **10**, 37–68.

Lettvin J. Y., Maturana H. R., McCulloch W. S. and Pitts, W. H. (1959) What the frog's eye tells the frog's brain. *Proc. IRE.* **47**, 1940–1959.

Ratliff F. (1965) *Mach Bands* Holden-Day, San Francisco.

Rodieck R. W. and Stone J. (1965) Analysis of receptive fields of cat retinal ganglion cells. *J. Neurophysiol.* **28**, 833–849.

Spinelli D. N. (1966) Visual receptive fields in the cat's retina: complications. *Science, N.Y.* **152**, 1768–1769.

Spinelli D. N. (1967) Receptive field organization of ganglion cells in the cat's retina. *Exp. Neurol.* **19**, 291–315.

Stevens S. S. (1970) Neural events and the psychophysical law. *Science, N.Y.* **170**, 1043–1050.

Tzanakou E. and Harth E. (1973) Determination of visual receptive fields by stochastic methods. *Biophys. Soc. Abst.* **13**, 42a.